Journal of the Korean Electrochemical Society
Vol. 28, No. 1, 2025, 14-23
https://doi.org/10.5229/JKES.2025.28.1.14

Supporting Information
pISSN 1229-1935
eISSN 2288-9000

Water-enriched WO_3 Nanostructures for Electrochromic Energy Storage and Photovoltaic Cell Integrated Electrochromic System

Aryal Krishna Prasad and Kwang-Soon Ahn*

School of Chemical Engineering, Yeungnam University, Gyeongsan 712-749, South Korea

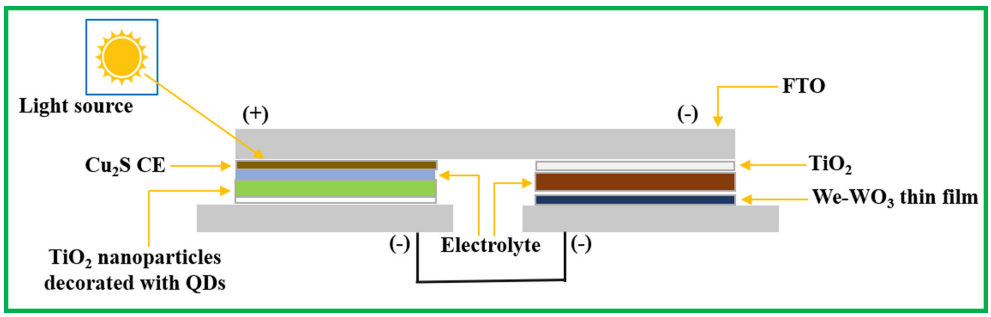

Fig. S1. Schematic arrangement of QDSSC-assisted We-WO_3 integrated device.

Table S1. Resistance parameters and electrochemical active area (EASA) from electrochemical impedance spectroscopy (EIS) analysis

Samples	R_s (Ω)	R_{ct} (Ω)	EASA (cm^2)	ΔE (V)
WO_3	8.4	25.3	0.0014	0.30
We-WO_3	7.5	20.5	0.0021	0.25

Table S2. Electrochromic parameters of ECD-WO_3 and We-WO_3 films measured at 750 nm

Samples	t_b (s)	t_c (s)	ΔT (%)	CE (cm^2/C)
WO_3	3.4	5.2	56.7	75.3
We-WO_3	1.6	3.3	73.6	93.1

*E-mail: kstheory@ynu.ac.kr (K.-S. Ahn)

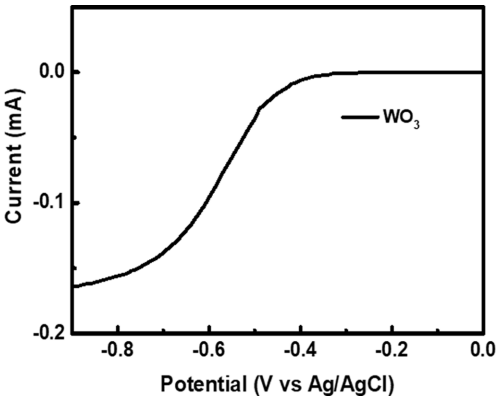

Fig. S2. Linear sweep voltammetry curves of WO_3.

An aqueous solution of 0.1 M $Na_2WO_4 \cdot 2H_2O$ was prepared and pH-adjusted to 1.0 for use in the LSV measurement of WO_3 (Fig. S2). Based on the LSV results, a constant potential of −0.8 V is confirmed for fabricating the WO_3 and We-WO_3 films over the ITO surface.

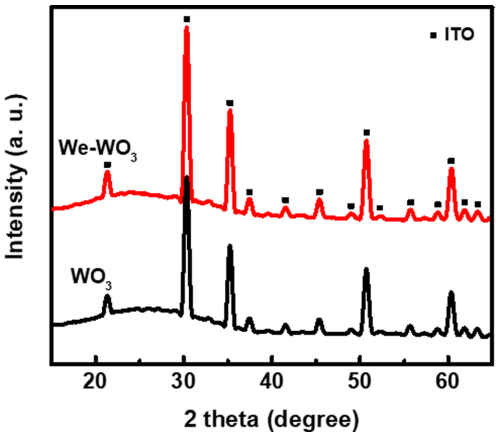

Fig. S3. XRD patterns of WO_3 and We-WO_3 thin films.

To investigate the crystalline nature of the WO_3 and We-WO_3 films, XRD measurements were performed, and the results are presented in Fig. S3. No diffraction peaks were observed for either film. The various peaks observed in the figure originate from the ITO surface. This suggests that both fabricated films are amorphous in nature.

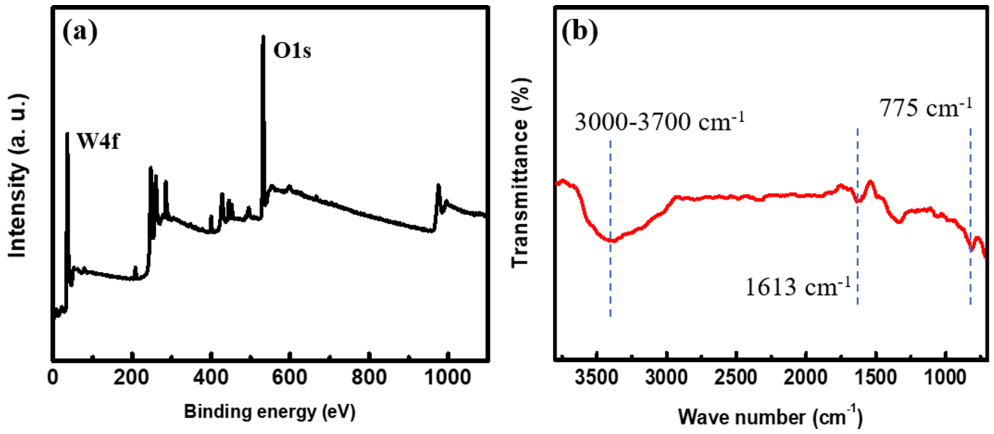

Fig. S4. (a) XPS survey and (b) FTIR spectra of We-WO_3 film.

The XPS survey spectrum of the We-WO_3 film reveals atomic compositions of 17.1% W and 82.9% O (Fig. S4a). To confirm the enhancement of the water content of We-WO_3, FTIR measurements were performed. This revealed the presence of hydrophilic groups, where a broad band appeared in the wavelength range of 3000–3700 /cm due to the O–H stretching vibration of the adsorbed water, as shown in Fig. S4b. Additionally, the band at 775 /cm is characteristic of W–O bonding.

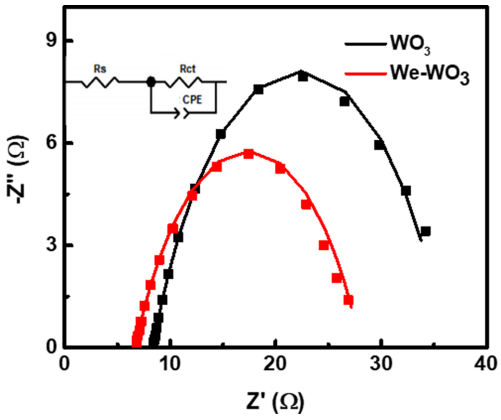

Fig. S5. Impedance measurement for WO_3 and We-WO_3 thin films.

The Nyquist plots for both films were obtained using impedance measurements, as shown in Fig. S5. Notably, We-WO_3 demonstrated the minimum charge-transfer resistance (R_{ct}) and series resistance (R_s) of 20.5 Ω and 7.5 Ω, respectively. On the other hand, the WO_3 film electrode exhibited an R_{ct} of 25.3 Ω and an R_s of 8.4 Ω. The results are summarized in Table S1. The overall electrochemical performance of We-WO_3 was attributed to improved charge transfer. Additionally, the minimal R_s value could be attributed to the enhanced active surface area resulting from the dispersed and exposed morphologies.

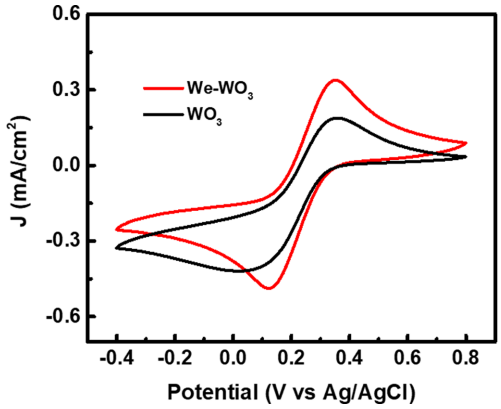

Fig. S6. CV data acquired in 0.1 M $[Fe(CN)]^{3-}$ for WO_3 and We-WO_3 thin films.

To calculate the electrochemical active surface area (EASA) of both films, CV was performed in 0.1 M $[Fe(CN)]^{3-}$, as shown in Fig. S6. The Randles–Sevcik equation was employed to calculate the EASA. We-WO_3 exhibited a higher EASA of 0.0021 cm^2, compared to WO_3 (0.0014 cm^2). In addition, We-WO_3 also possessed a minimum peak separation (ΔV) between the oxidation and reduction peaks, as seen in the above CV curve. This indicates that the surface of We-WO_3 is more suitable for the movement of ions during the electrochemical process.

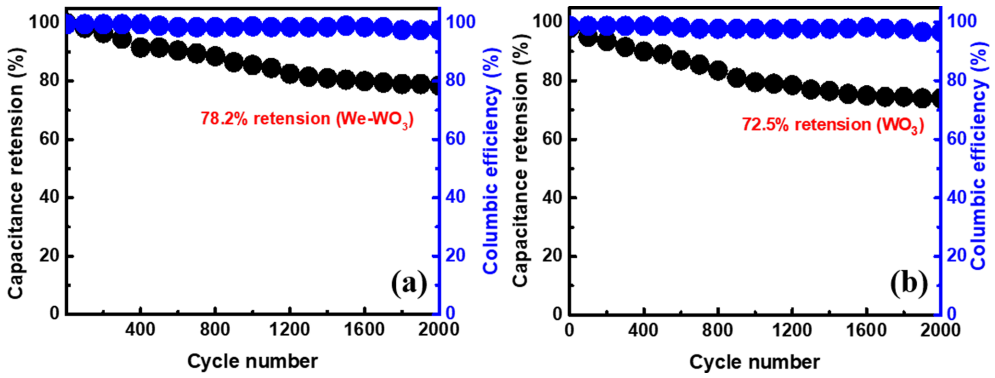

Fig. S7. Cyclic performance and coulombic efficiency of (a) We-WO_3 and (b) WO_3 thin films.

The capacitance retention (%) and coulombic efficiencies were measured for the We-WO_3 and WO_3 thin film electrodes at a current density of 5 mA/cm^2 in the potential range of −0.9–0.7 V. Based on the charge/discharge measurements up to 2000 cycles, We-WO_3 and WO_3 possess capacitive retentions of 78.2% and 72.5%, respectively. In addition, We-WO_3 exhibited a coulombic efficiency of >95%, suggesting good reversibility.